



## Face Recognition in Thermal Images based on Sparse Classifier

M. Shavandi<sup>a</sup>, I. E. P. Afrakoti<sup>\*b</sup>

<sup>a</sup> Faculty of Electrical Engineering, Hadaf Institute of Higher Education, Sari, Iran

<sup>b</sup> Faculty of Technical and Engineering, University of Mazandaran, Babolsar, Iran

### PAPER INFO

#### Paper history:

Received 16 November 2018

Received in revised form 28 December 2018

Accepted 03 January 2019

#### Keywords:

Face Recognition

Sparse Representations Classification

Thermal images

Norm  $\ell^0$

### ABSTRACT

Despite recent advances in face recognition systems, they suffer from serious problems because of the extensive types of changes in human face (changes like light, glasses, head tilt, different emotional modes). Each one of these factors can significantly reduce the face recognition accuracy. Several methods have been proposed by researchers to overcome these problems. Nonetheless, in recent years, using thermal images has gain more attention among the introduced solutions as an effective and unique solution. This article studies the performance of sparse processing techniques when facing with challenges of face recognition problem in thermal images. Also, the potential of the sparse classifier algorithm to receive information directly from input images without using any feature extraction algorithms was studied. The obtained results indicated that the sparse processing techniques outperform the Eigenface and KNN algorithms in terms of addressing the challenges of thermal images. In this work, USTC NVIN and CBSR NIR face datasets were used for simulation purposes. These datasets include the images with different emotional states (sad, happy, etc.) captured in different light conditions; also the images are captured both with and without wearing glasses. Simulation results have shown that sparse classifier can be an effective algorithm for the face recognition problem in thermal images.

doi: 10.5829/ije.2019.32.01a.10

## 1. INTRODUCTION

Face recognition as one of the most active biometric features has been considered by researchers. Face recognition methods based on visible light spectrum images have achieved considerable developments and practical successes. However, these systems encounter serious challenges in real ambients, such as light, glasses, makeup, head tilt, various emotional states etc, each of which alone can significantly reduce the recognition accuracy. Different solutions have been proposes in the literature to address these challenges. Using thermal images rather than visible images is a solution that has attracted attention of many scholars. This is because of various advantages of the former over the latter. Thermal images are produced based on sensitivity of infrared cameras to thermal alterations of the face. Formation of thermal images depends on intrinsic features of the face. Hence, given that the thermal energy of Long wave IR (LWIR) and Medium wave IR (MWIR) images is high, their formation does not require any external light sources

[1], while in Near IR (NIR) and Short wave IR (SWIR) sub-bands, it needs appropriate ambient light.

Among the advantages of thermal images over visible images is that they are more robust against light alterations [2]. Also, Friedrich and Yeshurun [3] stated that IR images are less affected by face or state changes. As as it was reported by Kakkirala [4], thermal images are less influenced by dust and smoke in the ambient. Another advantage is that temperature distribution in synthetic hair and skin differs from that of the natural hair and skin [1], which distinguishes these two types of images and makes the system more robust against deception.

Using thermal image for face recognition suffers from some problems, and the challenges have to be dealt with to achieve a reasonable recognition rate. Among these problems is sensitivity of LWIR and MWIR images to the ambient temperature, such a problem is true about emotional, physical and health conditions which may alter the body temperature. Also, alcohol consumption affects the thermal images. Glasses are another problem

\*Corresponding Author Email: [i.esmaili.p@umz.ac.ir](mailto:i.esmaili.p@umz.ac.ir) (I. E. P. Afrakoti)

to mention, because they are blurred in most of IR spectrums (LWIR, MWIR and SWIR) [5], which makes the loss of some important parts of the image, since this is the place of eyes which includes valuable information. samples thermal images and visible images are shown in Figure 1.

One of the first efforts to use infrared data for face recognition was carried out by Cutler [6]. His method was based on the well-known Eigenface technique. In this method, a 96% recognition accuracy was achieved. After that, many developed algorithms used the Eigenface as the basic classifier [1]. Majumder, and Bhowmik [7], have applied linear kernel support vector machine (LK-SVM) for image classification. Zhang et al. [8] used Convolutional Neural Network (CNN) neural network to classify the thermal images. They employed PolyU-NIRFD database which includes NIR images. In this paper, CNN directly receives the input images. The authors reported interesting results regarding the function of the system versus different factors. Wu et al. [9] used CNN for image classification. In their work, CNN classification algorithm directly obtains the features from input images. They evaluated the proposed system against factors such as head tilt, different face states, and light (illumination). They reported that the performance of their system is desirable. Zhao et al. [10] used the places (positions) of pupils to record faces. Then, they classified images using support vector machine algorithm. Zhao et al. achieved an accuracy of 79.6 percent. Cho et al. [11] evaluated the performance of several methods of machine learning algorithm in their research. They believed that the function of Radial Basis Function (RBF) classifier is more appropriate than that of other classifiers. Seal et al. [12] presented an approach based on vascular network information of thermal images. They carried out simulations using a personal database and classified the images using the neural network algorithm. Maximum recognition rate reported by Seal et al. [12] was 91.47%. Also, Awedat et al. [13] used the sparse representation classification based on integration of  $l^1$  and  $l^2$  norms. They evaluated the function of their system on two databases of visible images.

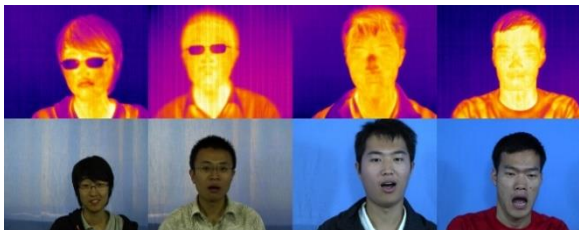


**Figure 1.** Some samples of thermal and corresponding visible images

Their system outperformed the popular classification algorithms such as K-Nearest Neighbor (KNN) and Support Vector Machines (SVM), even without using any feature extraction algorithms. Several studies [8, 9] showed that a powerful classification along with a simple feature extraction algorithm can result in a desirable function of the system. As can be observed in literature [8, 9, 13], some classification algorithms are able to directly extract information from input images. Reihanian et al. [14] used the composition of thermal and visible images for image recognition. They evaluated their work on two datasets including USTC.NVIN database. They used the sparse algorithm for image classification. Their system had different parts including filters, feature extractor, group classifier etc.

In this paper, the function of sparse processing classification algorithm in thermal face recognition is studied. To this end, the sparse processing classification algorithm is directly applied on the thermal input images. Also, USTC.NVIN and CBSR NIR Face Dataset databases are utilized for simulations. Results showed that the algorithm has a reasonable performance in dealing with challenges including different face states, the images with and without glasses as well as the noise. In section 2, the sparse classification based on linear sparse representation is presented according to literature [15]. Moreover, finding a sparse solution through minimizing normed zero-norm ( $l^0$ ), orthogonal matching pursuit (OMP) and sparse representation steps were studied. In section 3, datasets used in this paper are introduced, and in section 4, simulation results are provided.

## 2. CLASSIFICATION BASED ON SPARSE REPRESENTATION

The main problem in object detection is to correctly find the class of test data using training labeled data related to  $k$  separate classes. Training data of the  $i$ -th class as the columns of matrix  $A_i$  are defined as follows [16]:

$$A_i = [v_{i,1}, v_{i,2}, \dots, v_{i,n_i}] \in \mathfrak{R}^{m \times n_i} \quad (1)$$

where  $m$  is the number of features of each training sample and  $n_i$  is the number of samples in class  $i$ . In face recognition, columns of an image with dimensions of  $w \times h$  sequentially replace matrix columns. Thus, columns of  $A_i$  are training face images related to the  $i$ -th person. Assume that the training samples of each class form a sub-space, then each new test vector of class  $i$  can be written approximately as a linear combination of vectors of training samples related to class  $i$  as follows:

$$y = \alpha_{i,1}v_{i,1} + \alpha_{i,2}v_{i,2} + \dots + \alpha_{i,n_i}v_{i,n_i} \quad (2)$$

where  $y$  is the new data of class  $i$  and coefficients  $\alpha_{i,j}$  are real scalar values as  $j = 1, \dots, m$  that determine the weight of each vector. Since the class of  $i$ -th sample is not determined, we define the matrix  $A$  including all training vectors through putting together all  $A_i$  s as follows:

$$A = [A_1, A_2, \dots, A_k] \in \mathfrak{R}^{m \times n} \quad (3)$$

Now, the vector of the test sample  $y \in \mathfrak{R}^m$  can be represented by a linear combination of all training vectors as follows:

$$y = Ax_0 \in \mathfrak{R}^m \quad (4)$$

where vector  $x_0$  represents vector  $y$  in  $A$  space, and ideally all members of  $x_0$  except for coefficients of  $i$ -th class are equal to zero. Then, the vector of coefficients,  $x_0$ , can be represented as follows:

$$y = Ax_0 \in \mathfrak{R}^m \quad (5)$$

In face recognition,  $y = Ax$  is usually underdetermined (i.e.  $m < n$ ), so it does not provide a unique solution. In this case, a unique solution can be found by adding some conditions to the problem. As shown in Equation (5), most of the members of  $x_0$  vector are ideally zero. In this condition, one can select a solution among infinite number of solutions as the unique solution by adding  $\ell^0$  norm minimization condition. Zero norm means the number of non-zero elements. Therefore, to find the unique solution of  $y = Ax$ , it is suggested by Mohimani et al. [16] to solve the following optimization problem:

$$(\ell^0)\hat{x}_0 = \arg \min \|x\|_0 \text{ s.t. } y = Ax \quad (6)$$

where  $\|\cdot\|_0$  is zero-norm  $\ell^0$ .

## 2. 1. Find Sparse Solution by Minimizing Normed Zero-norm ( $\ell^0$ )

The use of smoothed zero-norm algorithm is a method to find the sparse solution. Since the zero-norm of a vector is discontinuous, a smooth function (7) is used in this method to approximate  $\ell^0$  norm of the vector  $x$ , which is an approximation of  $\ell^0$  norm [16]:

$$\|x\|_0 \approx m - \sum_i \exp\left(\frac{-x_i^2}{2\sigma^2}\right) = m - F_\sigma(x) \quad (7)$$

In these relations  $i$  is data class and  $y$  is new data belonging to  $i$  class.  $x_0$  vector defines  $y$  vector in  $A$  space which in ideal condition, all  $x_0$  members except coefficients related to  $i$ th class are zero.  $F_\sigma$  is smooth function of  $\ell^0$  norm approximation and  $\sigma$  estimated state of approximation. Equation (7), for small values of  $\sigma$ , when  $\sigma$  approaches zero, inequality converts to equality. Then, we can find the minimum solution through maximizing  $F_\sigma(x)$  for small values of  $\sigma$ . Here, the value of  $\sigma$  determines smoothness of the function  $F_\sigma(x)$ . The

more smaller is  $\sigma$ , the smoother is the  $F_\sigma(x)$ . Then, for small  $\sigma$ ,  $\ell^0$  norm can be minimized by maximizing the function  $F_\sigma(x)$ . As a result, the optimization problem is as follows:

$$(s\ell^0)\hat{x}_0 = \arg \min F_\sigma(x) \text{ s.t. } y = Ax \quad (8)$$

It is worth mentioning that in case the function is not smooth enough, the optimization problem may have many local minima for members of a vector. In order to find solutions of the optimization problem, the Steepest Ascent algorithm is used. Details of this algorithm called SL0 algorithm, are explained in literature [16]. Fast conversion is an important feature of SL0.

## 2. 2. Fine Sparse Solution Using Orthogonal Matching Pursuit

One of the most popular techniques to find sparse solution is the OMP. In fact, this is a modification of the matching pursuit (MP) algorithm. MP is among greedy algorithms, i.e. in each step attempts to make the best possible choice. In this method, the system tries to determine the coefficient of one atom in each step. In other words, it selects an atom with maximum similarity to the test sample, then calculates its coefficient. In the next step, the rest of test signal and the first atom are compared with the remaining atoms; again, the most similar atom is selected. In this way, the coefficient of one atom is determined in each step until the remaining norm is less than a threshold. In the MP method, when the best coefficient is selected, in next steps the previous coefficient cannot be discarded after selecting other coefficients. Therefore, perfect reconstruction of the signal is impossible in this algorithm, because the system is probable to make a wrong choice and devote the other choices for the amendment of this mistake. This may lead to a departure from the main sparse solution. In the OMP, after determining a new atom in each step, the linear combination of all atoms already selected is calculated. This reduces the error in test signal reconstruction. In general, the OMP is faster than the MP. It is appropriate to refer to literature [17] and [18] for more details.

## 2. 3. Sparse Representation Classification

For any new test sample  $y$ , the sparse representation of  $\hat{x}_0$  has to be obtained. Ideally, given that non-zero elements are the columns of the  $i$ -th class, it is simply possible to estimate  $x_0$  through assigning the test sample  $y$  to that. Nevertheless, it is not practical due to errors such as noises caused by non-zero elements of other classes, although with small values. Due to this problem, a variety of classifiers have been presented. One preliminary method is to choose a class with the largest non-zero elements as the true class. A more reasonable technique was presented by Wright et al. [15] in which we seek for a linear combination of the training samples of a class which provides a better estimation of the test sample  $y$  through

coefficients obtained from sparse representation. See Equation (9):

$$\min_i r_i(y) = \min_i \|A - y\delta_i(\hat{x}_0)\|_2 \quad (9)$$

Where to define the vector  $\delta_i(\hat{x}_0)\mathcal{R}^n$  for each class  $i$ , we have to set the elements corresponding to other classes equal to zero. Here, classification of  $y$  is based on the best estimation, and finally, a class with the least estimation error is selected as the true class. Figure 2 shows general identification steps face recognition in thermal images.

### 3. DATABASE

In this paper two databases are exploited for simulations, each of which is briefly described in the following.

**3. 1. USTV.NVIE Database** USTV.NVIE database consists of both thermal and visible images. Images of each person are captured in different face states (sadness, happiness, anger etc) with and without glasses, and with light radiation from front, right, and left sides. In this paper, 85 human image samples were used. For each person, there are six images in different states, without glasses and with front-side light radiation. Five images are also selected for leftside and right-side light radiations. In total, 16 images without glasses and 16 images with glasses were chosen.

**3. 2. CBSR NIR Face Dataset** This dataset includes NIR face images of 197 individuals captured in different emotional states, with and without glasses and with a trivial head tilt. For the simulation case without glasses, the images of 110 individuals, 20 samples for each person, were used. Due to the lack of image samples for all people in the dataset, for the case with glasses, only images of 48 individuals, 7 samples for each one, were used.

### 4. SIMULATION RESULTS

Simulation results have been analyzed separately on two databases. In all steps, 70% of images were used as training data and the the remaining 30% are assigned to test data.

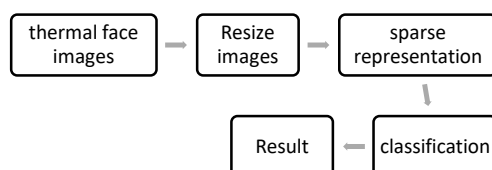


**Figure 2.** General identification steps of face recognition in thermal images

In all steps of simulations, at first all image formats were converted to gray. All classification algorithms were again simulated by the authors, and contents of the tables are not duplicated. The important point is the use of databases including a large number of images. Therefore, 1360 images from USTC-NVIE database [19] and 2200 images from CBSR NIR [20] Face Dataset database were used (although for some parts of the test such as images with glasses fewer images were used, due to incompleteness of the database). Whereas, other works in face recognition field have used limited datasets [3, 11, 21-23]. The use of a large number of samples has led to increased reliability of the results.

**4. 1. Simulation of USTV.NVIE Database** In each step of simulations, the results are obtained and analyzed on 240\*304 images. In the first part, the functions of OMP and normed  $\ell^0$  algorithms on thermal images with and without glasses have been considered. Next, the results were compared with those of Eigenface and KNN methods. Then, they were resized (shrunk) to 30\*40 and then we applied algorithms. Finally, after applying the Generalized singular value decomposition (GSVD) [24] algorithm on 30\*40 images and resizing (shrinking) the images to (1\*85), simulation results were analyzed. For images with and without glasses, the total 16 images captured in different emotional and light conditions, were used. The results are summarized in Table 1.

As shown in Table 1, there is a little difference between sparse processing methods with Eigenface and KNN on the images with and without glasses and with the image size of 69920 and 1200. By decreasing the image size to 85, sparse processing classification algorithms show a function near to that of KNN, but they outperform the Eigenface algorithm.

**TABLE 1.** Comparison between images with glasses, without glasses, and with and without glasses

Algorithm	w * h	with_glasses	without_glasses	without & with
$\ell^0$	69920	98.6	98.3	<b>98.9</b>
	1200	98.0	97.7	97.1
	85	89.4	91.7	84.4
OMP	69920	<b>98.7</b>	<b>98.7</b>	98.5
	1200	98.3	<b>98.7</b>	98.3
	85	88.0	89.8	81.7
KNN	69920	97.9	97.9	98.3
	1200	97.0	97.3	96.4
	85	93.1	87.0	87.1
Eigenface	69920	98.4	98.6	98.8
	1200	98.5	98.4	97.4
	85	2.3	2/7	3.4

In the second part of simulations, salt & pepper and Gaussian noises are applied to the images in 5 steps, then robustness of sparse algorithms is compared to those of the Eigenface and KNN methods. The image samples with salt & pepper and Gaussian noises are shown in Figures 3 and 4, and the corresponding results in Tables 2 and 3, respectively.

Tables 2 and 3 show the robustness of the sparse algorithms against noises. After increasing the variance of Gaussian noise up to 0.2, the functions of Eigenface and KNN algorithms are not satisfying. While both sparse algorithms have a reasonable performance after increasing the noise variance up to 0.3. Similarly, after applying the salt & pepper noise and increasing its level up to 0.4, Eigenface and KNN algorithms suffer a big drop in their performance, while both sparse algorithms show a desirable function.

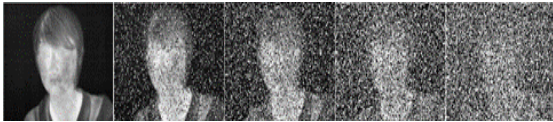


**Figure 3.** Applying salt & pepper noise in 5 steps. Level of noise from left to right is 0, 0.2, 0.4, 0.6 and 0.8.



**Figure 4.** Applying Gaussian noise in 5 steps. Noise variance is varying from 0 to 0.4 with step 0.1 respectively

**TABLE 2.** Comparison of different algorithms after applying salt & pepper noise and increasing its level in 5 steps

Algorithm	w * h	Level of noise				
		0	0.2	0.4	0.6	0.8
$\ell^0$ (proposed)	69920	98.3	<b>98.6</b>	<b>96.4</b>	<b>18.2</b>	1.3
OMP (proposed)	69920	<b>98.7</b>	98.1	95.4	2.1	1.2
Knn	69920	97.9	96.8	67.9	12.9	<b>2.4</b>
Eigenface	69920	98.6	95.6	69.9	13.7	2.2

**TABLE 3.** Comparison of the functions of different algorithms after applying Gaussian noise with variance of 0 to 0.4 with step 0.1

Algorithm	w * h	Noise variance				
		0	0.1	0.2	0.3	0.4
$\ell^0$ (proposed)	69920	98.3	98.6	<b>97.9</b>	<b>94.5</b>	<b>17.6</b>
OMP(proposed)	69920	<b>98.9</b>	<b>98.8</b>	96.8	76.9	4.7
Knn	69920	97.9	96.7	34.7	9.8	2.0
Eigenface	69920	98.6	97.2	37.3	9.3	2.7

In the next part, Interlaced Derivative Patterns (IDP) algorithm [25] was used for feature extraction. Then, the sparse algorithm is applied to the feature vector in the first step. In the second step, we placed the feature matrix of each image in the sequel of that, and then applied the sparse algorithm. Figure 5 shows the image after applying IDP. The results are summarized in Table 4.

As shown in Table 4, IDP feature extraction algorithm had no significant effect on the system function.

In the next step, Canny edge detection algorithm was used to extract the edges of the images. In the first step, the sparse algorithm is applied to the main image as well as to the edge image. In the next step, the edge image of each picture was placed in sequel of its main image. Then the sparse algorithm was applied. An edge detection image along with a mixture of the main image with the edge image are illustrated in Figure 6. The results summarized in Table 5 show that Canny edge detector has no significant effects on the applied algorithms.

**4. 2. Simulation of CBR NIR Face Dataset** In this dataset, mage size is 480\*640 which we resized them to 240\*320 and studied the functions of mentioned algorithms on these resized images.

In the first part, the function of sparse algorithm was studied on the images with and without glasses.



**Figure 5.** (a) Image after applying IDP and (b) the input thermal image

**TABLE 4.** Results of applying IDP on the image in two different states

	w * h	$\ell^0$	Eigenface	KNN	OMP
IDP	69920	<b>97.9</b>	97.4	97.6	97.6
[IM;IDP]	139840	<b>98.9</b>	98.8	98.4	<b>98.9</b>



**Figure 6.** Main image, edge image and the mixture of two images

**TABLE 5.** Results of applying Canny edge detector on the images in two states

	w * h	$\ell^0$	Eigenface	KNN	OMP
IM+canny	69920	98.4	97.8	97.6	<b>98.7</b>
[IM;canny]	139840	<b>98.9</b>	97.8	97.7	98.5

Then, the results were compared to those of Eigenface and KNN methods. For the case without glasses, the images of 110 individuals, 20 samples per person, and for the case with and without glasses, the images of 48 persons, 7 without and 7 with glasses samples for each one, were employed. The results are listed in Table 6.

As seen in Table 6, in NIR images of this dataset, sparse algorithms are obviously superior to the Eigenface and KNN algorithms, specially for the case with glasses.

In this step, salt & pepper and Gaussian noises are applied to the images, separately. Then, a comparison is drawn between the robustness of sparse processing algorithms and those of the Eigenface and KNN algorithms. The results are given in Tables 7 and 8, respectively.

As seen in Tables 7 and 8, the sparse algorithm shows a desirable function after applying both salt & pepper and Gaussian noises to NIR images. Therefore, after increasing the average value of Gaussian noise up to 0.1, both KNN and Eigenface algorithms experience a significant drop in their performance, while the function of sparse algorithms is yet desirable by the increased noise.

**TABLE 6.** Comparison of results obtained from images with glasses, without glasses, and without & with glasses

	Eigenface	KNN	$\ell^0$	OMP
without_glasses	91.8	89.1	97.7	<b>98.2</b>
without & with	94.3	90.0	96.8	<b>98.1</b>
with_glasses	88	86/7	96.0	<b>96.5</b>

**TABLE 7.** Comparison of different algorithms in the presence of salt & pepper noise and increasing the level of noise in 4 steps

Algorithm	Noise level			
	0.1	0.2	0.3	0.4
Eigenface	96.8	87.4	42.4	18.6
KNN	94.7	83.3	40.3	18.5
$\ell^0$	97.2	94.6	87.8	46.0
OMP	98.2	97.6	96.4	90.3

**TABLE 8.** Comparison of different algorithms in the presence of Gaussian noise with variance of 0.1 and increasing its average in 4 steps

Algorithm	Noise average			
	0.05	0.1	0.15	0.2
Eigenface	95.5	60.0	27.2	12.6
KNN	91.1	60.0	28.0	13.1
$\ell^0$	97.6	96.7	94.0	88.7
OMP	97.7	97.5	97.1	96.6

## 5. CONCLUSION

In this article, the functions of face recognition systems based on sparse classifier in thermal images were studied. Normed  $\ell^0$  and OMP algorithms were used to solve the sparse problem. Then, the system's function was investigated against different challenges of thermal image recognition (including different emotional states, glasses, noise etc). Simulation results show the superiority of the OMP and normed  $\ell^0$  to Eigenface and KNN algorithms. This superiority is more obvious in the presence of noise.

In the future work, the authors of this article will investigate the performance of sparse algorithms in the systems using both thermal and visible images. Also, they will study the effectiveness of the sparse algorithm against other challenges of face thermal images (including head tilt and ambient temperature), which are of great important in face recognition.

## 6. REFERENCES

- Ghiass, R.S., Arandjelovic, O., Bendada, H. and Maldague, X., "Infrared face recognition: A literature review", in Neural Networks (IJCNN), The 2013 International Joint Conference on, IEEE. (2013), 1-10.
- Mostafa, E., Hammoud, R., Ali, A., Farag, A.J.C.V. and Understanding, I., "Face recognition in low resolution thermal images", *Computer Vision and Image Understanding* Vol. 117, No. 12, (2013), 1689-1694.
- Friedrich, G. and Yeshurun, Y., "Seeing people in the dark: Face recognition in infrared images", in International Workshop on Biologically Motivated Computer Vision, Springer, Berlin, Heidelberg, (2002), 348-359.
- Kakkirala, K.R., Chalamala, S.R. and Jami, S., "Thermal infrared face recognition: A review", In *Computer Modelling & Simulation (UKSim), 2017 UKSim-AMSS 19th International Conference on.*, IEEE, (2017), 55-60.
- Kong, S.G., Heo, J., Abidi, B.R., Paik, J., Abidi, M.A.J.C.V. and Understanding, I., "Recent advances in visual and infrared face recognition—a review", *Computer Vision and Image Understanding*, Vol. 97, No. 1, (2005), 103-135.
- Cutler, R.G., "Face recognition using infrared images and eigenfaces", **University of Maryland**, (1996).
- Majumder, G. and Bhowmik, M.K., "Gabor-fast ica feature extraction for thermal face recognition using linear kernel support vector machine", in Computational Intelligence and Networks (CINE), 2015 International Conference on, IEEE. (2015), 21-25.
- Zhang, X., Peng, M. and Chen, T., "Face recognition from near-infrared images with convolutional neural network", in Wireless Communications & Signal Processing (WCSP), 2016 8th International Conference on, IEEE, (2016), 1-5.
- Wu, Z., Peng, M. and Chen, T., "Thermal face recognition using convolutional neural network", in Optoelectronics and Image Processing (ICOIP), 2016 International Conference on, IEEE. (2016), 6-9.
- Zhao, S., Grigat, R.-R.J.M.L. and Recognition, D.M.i.P., "An automatic face recognition system in the near infrared spectrum", In *International Workshop on Machine Learning and Data Mining in Pattern Recognition*, Springer, Berlin, Heidelberg, (2005), 633-633.

11. Cho, S.-Y., Wang, L. and Ong, W.J., "Thermal imprint feature analysis for face recognition", in Industrial Electronics, 2009. ISIE 2009. IEEE International Symposium on, IEEE. (2009), 1875-1880.
12. Seal, A., Bhattacharjee, D., Nasipuri, M. and Basu, D.K., "Minutiae based thermal face recognition using blood perfusion data", in Image Information Processing (ICIP), 2011 International Conference on, IEEE. (2011), 1-4.
13. Awedat, K., Essa, A. and Asari, V., "Sparse representation classification based linear integration of l1-norm and l2-norm for robust face recognition", (2017).
14. Reihanian, S., Arbabi, E. and Maham, B., "Random sparse representation for thermal to visible face recognition", in Computers and Communications (ISCC), 2017 IEEE Symposium on, IEEE. (2017), 1380-1385.
15. Wright, J., Yang, A.Y., Ganesh, A., Sastry, S.S., Ma, Y.a. and intelligence, m., "Robust face recognition via sparse representation", *IEEE Transactions on Pattern Analysis and Machine Intelligence*, Vol. 31, No. 2, (2009), 210-227.
16. Mohimani, H., Babaie-Zadeh, M. and Christian J., "A fast approach for overcomplete sparse decomposition based on smoothed l<sup>0</sup> norm", *IEEE Transactions on Signal Processing*, Vol. 57, No. 1, (2009), 289-301.
17. Tropp, Joel A., and Anna C. Gilbert. "Signal recovery from random measurements via orthogonal matching pursuit." *IEEE Transactions on Information Theory*, Vol. 53, No. 12 (2007): 4655-4666.
18. Pati, Y.C., Rezaifar, R. and Krishnaprasad, P.S., "Orthogonal matching pursuit: Recursive function approximation with applications to wavelet decomposition", in Signals, Systems and Computers. 1993 Conference Record of The Twenty-Seventh Asilomar Conference on, IEEE. (1993), 40-44.
19. *Nvie database*. A Natural Visible and Infrared facial Expression Database; Available from: <http://nvie.ustc.edu.cn>.
20. *Cbsr nir face dataset*. OTCBVS Benchmark Dataset Collection; Available from: <http://vcip1-okstate.org/pbvs/bench/index.html>.
21. Martinez, B., Binefa, X. and Pantic, M., "Facial component detection in thermal imagery", *Computer Vision and Pattern Recognition Workshops (CVPRW)*, 2010 IEEE Computer Society Conference on, IEEE. (2010), 48-54.
22. Lin, Chun-Fu, and Sheng-Fuu Lin. "Accuracy enhanced thermal face recognition." *Infrared Physics & Technology*, Vol. 61 (2013), 200-207.
23. Farokhi, Sajad, Jan Flusser, and Usman Ullah Sheikh. "Near infrared face recognition: A literature survey." *Computer Science Review*, Vol. 21 (2016), 1-17.
24. Howland, Peg, Jianlin Wang, and Haesun Park. "Solving the small sample size problem in face recognition using generalized discriminant analysis." *Pattern Recognition*, Vol. 39, No. 2 (2006): 277-287.
25. Shobeirnejad, A. and Gao, Y., "Gender classification using interlaced derivative patterns", in Pattern Recognition (ICPR), 2010 20th International Conference on, IEEE. (2010), 1509-1512.

## Face Recognition in Thermal Images based on Sparse Classifier

M. Shavandi<sup>a</sup>, I. E. P. Afrakoti<sup>b</sup>

<sup>a</sup> Faculty of Electrical Engineering, Hadaf Institute of Higher Education, Sari, Iran

<sup>b</sup> Faculty of Technical and Engineering, University of Mazandaran, Babolsar, Iran

### PAPER INFO

چکیده

#### Paper history:

Received 16 November 2018

Received in revised form 28 December 2018

Accepted 03 January 2019

#### Keywords:

Face Recognition

Sparse Representations Classification

Thermal images

Norm  $l^0$

سیستم‌های شناسایی چهره علی‌رغم پیشرفت‌های بسیاری که داشته‌اند به دلیل طیف وسیع تغییرات چهره انسان (تغییراتی مانند: نور، عینک، چرخش سر، حالت‌های عاطفی مختلف) هنوز هم با مشکلاتی مواجه هستند. راه حل‌های مختلفی از سوی محققان جهت غلبه بر این مشکلات مطرح شده است، اما در سال‌های اخیر از بین این راه حل‌ها استفاده از تصاویر حرارتی به عنوان راه حلی موثر و خاص مورد توجه قرار گرفته است. در این مقاله به بررسی عملکرد روش‌های پردازش تنک در مواجهه با چالش‌های شناسایی تصاویر حرارتی چهره پرداخته شده است. همچنین توانمندی الگوریتم طبقه‌بند تنک در دریافت اطلاعات به صورت مستقیم از تصاویر ورودی بدون استفاده از هیچ گونه الگوریتم استخراج ویژگی مورد ارزیابی قرار گرفته است. نتایج بدست آمده از شبیه‌سازی حاکی از برتری روش‌های پردازش تنک نسبت به الگوریتم‌های KNN، Eigenface و CBSR NIR Face و USTC.NVIN در این کار از دو مجموعه داده‌ی Dataset جهت شبیه‌سازی استفاده شده است. تصاویر موجود در این پایگاه‌های داده شامل تصاویر با حالت چهره مختلف (غم، شادی و...)، که در شرایط نوری متفاوتی تهیه شده‌اند و همچنین تصاویر با عینک و بی‌عینک می‌باشد. نتایج شبیه‌سازی توانایی الگوریتم‌های تنک را در مواجهه با مساله شناسایی چهره در تصاویر حرارتی تایید می‌کند.

doi: 10.5829/ije.2019.32.01a.10